

Electron Acceleration in Nd-Laser Plasma Beat-Wave Experiments

F. Amiranoff,¹ D. Bernard,³ B. Cros,⁴ F. Jacquet,³ G. Matthieussent,⁴ P. Miné,³ P. Mora,⁵ J. Morillo,² F. Moulin,¹
A. E. Specka,³ and C. Stenz⁶

¹Laboratoire pour L'Utilisation des Laser Intenses, Ecole Polytechniques, Centre National de la Recherche Scientifique,
91128 Palaiseau, France

²Section d'Etude des Solides Irradiés, Commissariat à l'Energie Atomique, Ecole Polytechnique, 91128 Palaiseau, France

³Laboratoire de Physique Nucléaire et des Hautes Energies, Ecole Polytechnique, IN2P3, Centre National de la Recherche
Scientifique, 91128 Palaiseau, France

⁴Laboratoire de Physique des Gaz et des Plasma, Université Paris Sud, Centre National de la Recherche Scientifique,
91405 Orsay, France

⁵Centre de Physique Theorique, Ecole Polytechnique, Centre National de la Recherche Scientifique, 91128 Palaiseau, France

⁶Groupe de Recherches sur l'Energetique des Milieux ionisés, Université d'Orléans, Centre National de la Recherche Scientifique,
45000 Orléans, France

(Received 13 February 1995)

An electron beam has been accelerated in a plasma wave generated by the laser beat-wave method. The beating of two Nd-laser pulses at wavelengths close to 1 μm creates a relativistic plasma wave in a deuterium plasma. Electrons injected at an energy of 3 MeV are observed to be accelerated up to 3.7 MeV after the plasma. The energy gain is compatible with a peak electric field of the order of 0.6 GV/m, in agreement with model predictions. The experimental setup and the main results are presented.

PACS numbers: 52.75.Di, 41.75.Lx, 52.40.Nk

The generation of large electric fields in plasmas by high-power lasers has been studied for several years in the context of particle acceleration [1]. Among the proposed techniques, the beat-wave approach [2] has led to several experimental studies. In this technique, the beating between two laser beams with slightly different angular frequencies ω_1 and ω_2 excites a longitudinal oscillation in a plasma at the difference frequency $\delta\omega = \omega_1 - \omega_2$. If the natural oscillation frequency of the electrons in the plasma (the plasma frequency ω_p) is close to the difference frequency $\delta\omega$, the plasma oscillation is excited resonantly and can lead to large electric fields. The phase velocity of the longitudinal field, which is equal to the group velocity of the laser electromagnetic wave in the plasma, is very close to the speed of light, as the plasma density is very low. This longitudinal field may thus be used to accelerate relativistic particles to very high energies.

Beat-wave experiments using CO₂ lasers at wavelengths near 10 μm [3–5] or Nd lasers at 1 μm [6,7] have shown electric fields of the order of 1 GV/m or more. Nevertheless, the physics of the plasma wave is different in these two cases. In the CO₂ case, the saturation of the electric field is attributed to relativistic detuning that occurs when the oscillation velocity of the electrons is so high that the relativistic mass correction has to be taken into account and has to detune the plasma electrons from the pump beat-wave term. In the Nd case, two effects tend to lower the saturation level of the plasma wave. First, the pump term is proportional to λ^2 , the square of the mean wavelength of the lasers. At comparable laser intensities ($\approx 10^{15}$ W/cm²) this leads to a reduction of the pump term by a factor of

100. Second, present Nd experiments are performed in plasmas with a higher electron density than in CO₂ laser experiments ($n_e \approx 10^{17}$ cm⁻³ instead of 10^{16} cm⁻³). This leads to a much faster coupling by modulational instability between the beat-wave generated electron waves and ion waves, as has been shown in previous experiments [7,8].

It is not clear *a priori* which laser type is better suited for beat-wave acceleration. Nd lasers allow the generation of plasma waves with a higher Lorentz factor γ , which is desirable for acceleration of ultrarelativistic particles. On the other hand, in current experiments using Nd lasers, the growth of the plasma wave saturates at much lower amplitudes than for CO₂ lasers. While efficient acceleration of relativistic electrons injected into a plasma has already been reported in the case of CO₂ lasers [9,10], we report in this Letter the first acceleration experiment with Nd lasers.

The experimental setup is divided into two major sections. First, a beam of relativistic electrons and a laser beam with two different wavelengths are focused on the same axis and at the same point in a gas-filled vessel. Second, the energy spectrum of the accelerated electrons is measured and correlated with the presence of an intense longitudinal electric field. A schematic diagram of the setup is shown in Fig. 1, and a summary of the experimental parameters is listed in Table I.

The laser chain at LULI delivers two pulses at wavelengths 1.0642 and 1.0530 μm . This beam is then guided inside a vacuum pipe to the experimental area located 190 m away from the laser room. An optical relay consisting of a pair of 50 m focal-length lenses images the entrance window to the exit. Vacuum is necessary to

prevent refraction along the tube, while the optical relay maintains the size and the optical quality of the beam. The two pulses are then focused into a gas-filled vessel by a 1.5 m focal-length doublet lens. The measured difference between the wavelengths of the two pulses $\delta\lambda = 112 \pm 1.3 \text{ \AA}$ corresponds to a resonant electron density of $1.115 \times 10^{17} \text{ cm}^{-3} \pm 2.3\%$. The deuterium density in the vessel is adjusted with a precision of $\pm 0.3\%$. The laser focal spot, measured by an imaging system on exit, consists of a central spot $60 \pm 20 \text{ }\mu\text{m}$ in diameter (FWHM) and some outer rings. We estimate that the central spot contains about 50% of the laser energy thus giving the maximum intensities listed in Table I. After ionization of the gas by multiphoton ionization [7], the beating laser waves generate a primary, relativistic electron plasma wave which later decays into secondary electron and ion waves by modulational instability [7,8]. Part of the laser beam undergoes coherent Thomson scattering on these secondary waves and is detected at an angle of 5° with respect to the laser axis by a spectrometer and a streak camera. The scattered light intensity at $\omega_1 + \delta\omega$ is correlated to the amplitude of the primary plasma wave, and is used as an optical diagnostic that beat-wave generation actually takes place on each individual shot.

The focusing, alignment, and detection of the electron beam will be described in more detail in Ref. [11]. The electron source is a pulsed Van de Graaff accelerator delivering electrons with a kinetic energy of 2.500 MeV. The pulse duration has been set to 0.32 ms and the beam current during the laser shot is $170 \text{ }\mu\text{A}$. The electrons are focused on a $1.5 \text{ }\mu\text{m}$ thick aluminum foil separating the vacuum in the electron beam pipe from the deuterium gas in the vessel. After crossing the foil, the beam is brought on the laser axis by a triple

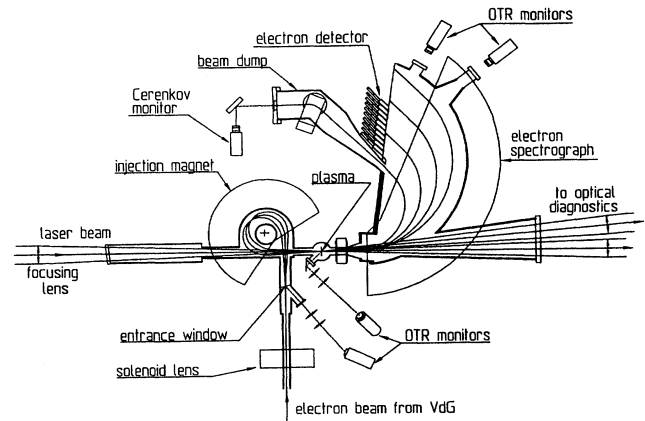


FIG. 1. Experimental setup.

focusing (i.e., stigmatic and achromatic) dipole magnet. The position and size of the electron beam are measured by beam monitors which detect optical transition radiation emitted by the electrons impinging on a metal surface [12]. The electron beam is monitored at four locations along its path. In order to ensure the (spatial and angular) coincidence of the electron and laser axes, the two beams are monitored at the plasma location and 3 cm behind this point. The electron spot size at focus is $25 \text{ }\mu\text{m}$ (rms) in vacuum and $45 \text{ }\mu\text{m}$ in 2 mbar of deuterium.

The energy spectrum of the electrons after passing the plasma is measured by a magnetic spectrograph consisting of a quadrupole-dipole combination and an array of 10 scintillators read by photomultiplier tubes (PMT). At the injection energy of 3 MeV, the spectrograph images the beam coming from the plasma stigmatically to the en-

TABLE I. Summary of the experimental parameters.

Laser beam	
Nd-YAG:	$\lambda = 1.0642 \text{ }\mu\text{m}$ $\tau = 200 \text{ ps}$ (FWHM) $E = 4.4 \text{ J}$ $I_{\text{max}} = 1.3 \times 10^{14} \text{ W/cm}^2$
Nd-YLF:	$\lambda = 1.0530 \text{ }\mu\text{m}$ $\tau = 90 \text{ ps}$ (FWHM) $E = 11.8 \text{ J}$ $I_{\text{max}} = 7.6 \times 10^{14} \text{ W/cm}^2$
Diameter:	65 mm Focal length: 1500 mm
Probe beam:	The probe beam is the Nd-YLF beam
Focal spot size:	$60 \pm 20 \text{ }\mu\text{m}$ (FWHM)
Electron beam	
Total energy:	3.011 MeV Energy fluctuation: $\Delta E/E = 10^{-3}$
Current:	$170 \text{ }\mu\text{A}$ i.e., $\approx 1000 \text{ e}^-/\text{ps}$
Focal spot:	in vacuum: $25 \text{ }\mu\text{m}$ (rms) in 2 mbar D_2 : $45 \text{ }\mu\text{m}$ (rms) i.e., $106 \text{ }\mu\text{m}$ (FWHM)
Divergence:	10 mrad (rms)
Gas and plasma:	
	deuterium
Resonant pressure:	2.272 mbar or 1.704 Torr at 22°C
Resonant electron density:	$1.115 \times 10^{17} \text{ cm}^{-3} \pm 2.3\%$ corresponding to $\delta\lambda = 112.0 \pm 1.3 \text{ \AA}$
Electron temperature:	$T_e \approx 20 \text{ eV}$ Debye length: $\lambda_D \approx 0.1 \text{ }\mu\text{m}$
Plasma wave	
Wavelength	$\lambda_p = 100 \text{ }\mu\text{m}$ Relativistic factor: $\gamma = 94.5$
Detection system:	
Lowest energy:	3.34 MeV Increment: 0.158 MeV Channel width: 0.150 MeV
Angular acceptance at 3.5 meV:	90 mrad (horizontal) 110 mrad (vertical)

trance of a beam dump, in order to reduce the background noise due to nonaccelerated electrons. Moreover, collimators are arranged along the path of the electrons to block large angle electrons in a clean way [11]. The residual noise in the detectors is due to electrons which scatter on the gas molecules inside the chamber and then backscatter from the edges of the dump entrance. This noise amounts to about $5 e^-/\text{ns}$, i.e., about 5×10^{-6} of the $1000 e^-/\text{ps}$ entering the chamber. The PMT signals are electronically gated with a 5-ns-long gate. The noise thus corresponds to about $25 e^-$ per channel. Two of the channels are continuously monitored on an oscilloscope for cross-check. Each signal consists of a long (millisecond) background noise plus a short (5 ns total width) signal associated with the electrons accelerated in the plasma. The uncertainty on the electron number is partly due to the calibration process ($\pm 15\%$) and partly to the statistical fluctuation of the noise from scattered electrons ($\pm 5 e^-$).

Accelerated electrons were measured in more than 80 successful laser shots. The total number and the energy spectrum of these electrons depend on many physical parameters such as laser intensity, time delay between the two pulses, gas pressure, relative position of electron, and laser focus. It is important to emphasize here that all these parameters are correlated in a nontrivial way. The instantaneous plasma density, for instance, depends not only on the initial gas density but also on the density evolution due to the ponderomotive force of the laser and of the plasma wave [13].

A number of null tests were performed, consisting of shots with either no electrons, no gas, a single laser wavelength, or two wavelengths separated in time. None of these shots showed a signal of accelerated electrons.

Under optimal conditions, we typically observe several hundred accelerated electrons at energies between 3.34 and 3.66 MeV, corresponding to the mean energies of the first three channels. Figure 2 shows the variation in the number of detected electrons as a function of the gas fill pressure, near the resonant pressure P_{res} . A significant acceleration is observed for gas pressures ranging from $0.97P_{\text{res}}$ to more than $1.04P_{\text{res}}$, whereas no electrons are measured below $0.97P_{\text{res}}$. We can also see in Fig. 2 that the number of electrons detected in channel 1 is fairly constant near the resonant pressure. On the contrary, the number of electrons which gain more energy shows much larger fluctuations. This can be explained by the large sensitivity of the maximum energy gain to the peak value and to the coherence of the accelerating electric field.

In Fig. 3, a relatively good correlation between the signal given by the optical diagnostic and the number of accelerated electrons can be observed. The presence of few shots showing a large Thomson-scattering signal and a small number of accelerated electrons may be due to some misalignment between the electron beam and the laser beam during the shot. While it is obviously difficult

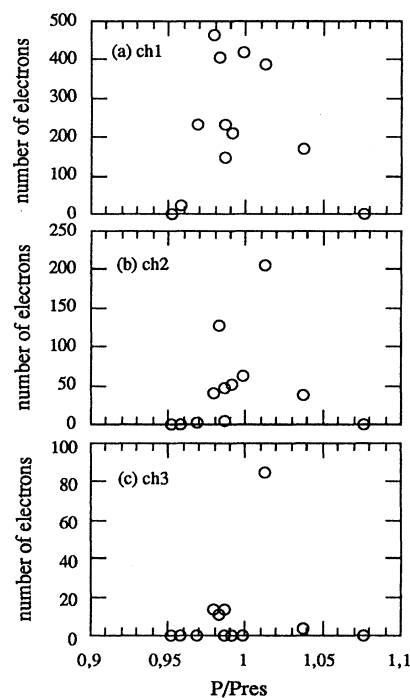


FIG. 2. Number of electrons detected in channel 1 (3.27–3.41 MeV), channel 2 (3.43–3.57 MeV), and channel 3 (3.59–3.73 MeV) as a function of the gas-fill pressure normalized to the resonant pressure indicated in Table I. In this series, the distance between the laser and electron foci is 7 mm.

to make a quantitative comparison between this indirect optical signal and the electron number, this correlation is additional evidence that the beat wave is responsible for the observed electrons.

In order to estimate the strength of the accelerating field, we compared the measured electron spectra with a simple 3D model [14]. In this model, we assume a plasma wave with an envelope corresponding to a Gaussian laser beam. The radial dependence is Gaussian with a focal spot size equal to the measured value. The longitudinal variation is Lorentzian with a Rayleigh length $L/2$. In order to take into account the saturation by modulational instability, we assume a plasma wave amplitude ramping linearly during 30 ps (see Fig. 6 of Ref. [8]). After this time, the modulational instability is believed to destroy the plasma wave and to stop the acceleration mechanism. All other parameters are those of Table I. The two free parameters are the Rayleigh length and the maximum electron density perturbation δ .

When the energy gain remains small, i.e., when the electron velocity does not change, the maximum value of the gain is given [15] by $\Delta W = \Delta W_0 e^{-L/l_d}$, where $\Delta W_0 = mc^2 \pi^2 \delta L / \lambda_p$ represents the integral of the electric field over the whole plasma length; and the second factor takes into account the phase slippage between the

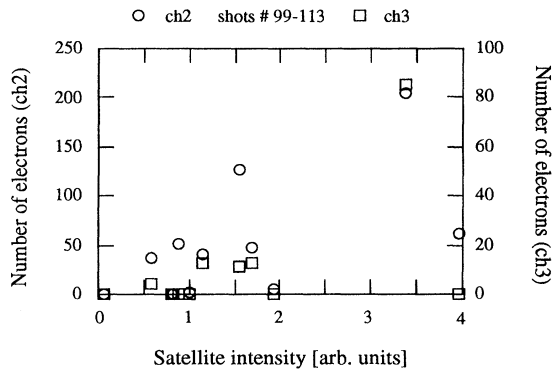


FIG. 3. Number of accelerated electrons as a function of the integrated intensity in the Thomson-scattering satellite on the same series of shots as in Fig. 2.

electron and the wave, i.e., the successive accelerating and decelerating phases explored by a slow electron injected in a high phase-velocity field. In our case [15] the dephasing length $l_d \approx 2.2$ mm. For a diffraction-limited beam, $L \approx 4.8$ mm, and the maximum observed energy gain of 0.7 MeV would lead to $\delta \approx 2.6\%$. In the case of a non-diffraction-limited beam, the longer Rayleigh length leads to an even higher maximum δ .

A comparison between measured and calculated electron spectra is shown in Fig. 4 for a Rayleigh length of 2.4 mm. The results of the best shots are compared with this model for a peak electron density perturbation $\delta = 1.6\%$, 2% , and 2.4% . A good agreement for the slope of the spectra is obtained for $\delta = 2\%$; whereas, the predicted absolute number of electrons is about 8 times the measured value. The maximum energy gain is slightly

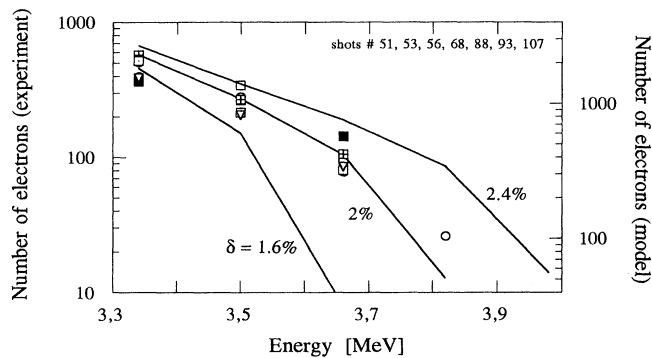


FIG. 4. Comparison between the best electron spectra and the results of the acceleration model for a peak plasma wave amplitude of $\delta = 1.6\%$, 2% , and 2.4% and a Rayleigh length of 2.4 mm. Each symbol represents the number of electrons per channel for one single shot, and the solid lines simply join the predicted values for the number of electrons in each channel. Except on one shot, no electrons were detected on channel 4. Note the difference of the factor of 8 in the vertical scales for experiment and model.

larger than predicted above, because the electron velocity changes during the acceleration and phase slippage is less important.

A number of physical aspects are not included in this simple model: the complex structure of the laser focal spot, the electron density variations in the plasma, the beat-wave growth time that depends on the local laser intensity, the coherence of the beat wave, and its evolution after saturation takes place. A detailed analysis of all these effects is out of the scope of this Letter, and some of them will be discussed in a future paper.

Acceleration of electrons has been reproducibly observed in a plasma beat-wave experiment using a Nd:glass laser. Electrons injected at an energy of 3 MeV have been accelerated up to 3.7 MeV. A preliminary analysis shows that this result is compatible with a peak plasma wave amplitude of 2% corresponding to a peak electric field strength of 0.6 GV/m. This value is also in good agreement with theoretical predictions, taking into account modulational instability, and with the experimental Thomson-scattering measurements [8].

We gratefully acknowledge the help of the technical staff of the LULI, LPNHE, and SESI during these experiments. This work has been partially supported by Ecole Polytechnique, IN2P3-CNRS, SPI-CNRS, CEA, EEC, and DRET.

- [1] *Advanced Accelerator Concepts*, edited by J.S. Wyrtele AIP Conf. Proc. No. 279 (AIP, New York, 1993).
- [2] T. Tajima and J.M. Dawson, Phys. Rev. Lett. **43**, 267 (1979).
- [3] C.E. Clayton, C. Joshi, C. Darrow, and D. Umstadter, Phys. Rev. Lett. **54**, 2343 (1985); F. Martin and T.W. Johnston, Phys. Rev. Lett. **55**, 1651 (1985).
- [4] F. Martin, J.P. Matte, H. Pepin, and N.A. Ebrahim, in *Proceedings of the Workshop on New Developments in Particle Acceleration Techniques, Orsay, 1987*, edited by S. Turner (Organisation Européenne pour le Recherche Nucléaire, Genève, 1987), p. 360.
- [5] Y. Kitagawa *et al.*, Phys. Rev. Lett. **68**, 48 (1992).
- [6] A.E. Dangor, A.K.L. Dymoke-Bradshaw, and A.E. Dyson, Phys. Scr. **T30**, 107 (1990).
- [7] F. Amiranoff *et al.*, Phys. Rev. Lett. **68**, 3710 (1992).
- [8] F. Moulin *et al.*, Phys. Plasmas **1**, 1318 (1994).
- [9] C.E. Clayton *et al.*, Phys. Rev. Lett. **70**, 37 (1993); C.E. Clayton, M.J. Everett, A. Lal, D. Gordon, K.A. Marsh, and C. Joshi, Phys. Plasma **1**, 1753 (1994).
- [10] N.A. Ebrahim, J. Appl. Phys. **76**, 7645 (1994).
- [11] F. Amiranoff *et al.*, Nucl. Instrum. Methods Phys. Res., Sect. A (to be published).
- [12] A.E. Specka *et al.*, in *Proceedings of the IEEE Particle Accelerator Conference Washington, D.C., 1993* (IEEE, New York, 1993), pp. 2450–2452.
- [13] J.R. Marquès *et al.*, Phys. Fluids B **5**, 597 (1993).
- [14] P. Mora, J. Appl. Phys. **71**, 2087 (1992).
- [15] P. Mora and F. Amiranoff, J. Appl. Phys. **66**, 3476 (1989).